Journal of Molecular Structure 934 (2009) 103–111

Contents lists available at ScienceDirect

Journal of Molecular Structure

journal homepage: www.elsevier.com/locate/molstruc

Conformational and electronic study of *cis*-peptides (non-proline residues) occurring in natural proteins

Lucas J. Gutierrez, Héctor A. Baldoni, Ricardo D. Enriz *

Departamento de Química, Universidad Nacional de San Luis, Chacabuco 917, 5700 San Luis, Argentina
Instituto de Matemática Aplicada San Luis, CONICET, Argentina
IMIBIO/SL-CONICET, Argentina

ARTICLE INFO

Article history:
Received 9 March 2009
Received in revised form 11 June 2009
Accepted 17 June 2009
Available online 30 June 2009

Keywords:
Conformational potential energy surfaces
Peptide model
Non-proline *cis*-peptide bonds
Ab initio
DFT calculations

ABSTRACT

First-principle computations were carried out on the conformational hyperspace of *cis*-peptide bond isomers of Ac-Gly-Gly-NHMe, Ac-Gly-Ala-NHMe, Ac-Ala-Gly-NHMe and Ac-Ala-Ala-NHMe. Using the concept of multidimensional conformational analysis (MDCA), geometry optimisations were performed at B3LYP/6-31G(d) level of theory, and single point energies were calculated at the B3LYP/aug-cc-pVDZ//B3LYP/6-31G(d) level of theory for the corresponding optimized structures. The relative stabilities of the various conformers were analysed using the theory of atoms in molecules. The theoretical results were compared with some experimental data (X-ray).

1. Introduction

In protein structures, the peptide bond conformation is found to be *trans* in the majority of cases [1]. Exceptions to this are the peptide bonds between any amino acid and proline, for which an appreciable fraction occurs in the *cis* conformation. It is clear that the *cis* form is energetically less stable, due to the steric repulsion of the two neighbouring C^{α} atoms, but the absolute numbers have been the basis of much debate. The planar peptide bond in proteins is known to occur predominantly in the *trans*-conformation (1). Planarity is thought to be maintained by a high rotational barrier due to partial double bond character [2–7]. Kang [8] reported that in the gas phase the rotational barriers to the *trans*-to-*cis* and *cis*-to-*trans* isomerizations for the non-prolylpeptide bond of the alanine dipeptide are estimated to be 19.81 and 15.02 Kcal/mol at the RHF/6-31G(d) level, respectively, and 19.66 and 15.63 Kcal/mol at the B3LYP/6-311++G(d,p) level, respectively. These barriers increase as the solvent polarity increases (12). Our own results for *N*-acetyl-l-prolin-*N*-methylamide indicate a range between 17 and 21 Kcal/mol in function of the molecular system using DFT [9] and *ab initio* calculations with extended basis set [10]. Recently it has been tried to spell out the residual conformational flexibility of Ac-$_{L}$Pro-NH_2 using matrix isolation IR and VCD spectroscopy in Ar and Kr matrices [11]. This study suggests that proline can at as a conformational lock, since the backbone predominantly adapts to the $t\gamma_{L}$ structure.

Due to the energy barrier, *cis–trans* isomerization of peptide bond is a rather slow process at room temperature and has been shown to play an important role in protein folding [12–17]. Interestingly, it has been noticed recently that *cis*-peptide bonds may play a more significant role in protein structures than was hitherto imagined. The analysis of protein data bank (PDB) revealed an unexpected number of *cis*-peptide bonds [18,19]. Even if proline *cis*-peptide bonds, which are the most abundant, are discounted an unexpectedly large number was still observed. There is mounting evidence [20,21] that *cis*-peptide bonds play significant biological roles in several areas even though their abundance is considerably minor with respect to the *trans*-isomer. Furthermore, it has been established that *cis*-peptide bonds may be both structural and functionally important [8]. For example it has been detected in breast tumour antibody (SM3) [22] and it has been found to play a role in protein folding and unfolding [23]. Several studies on the non-prolyl *cis–trans* isomerization of mutant proteins, in which prolines are replaced by alanines or other residues, have been carried out to explore the role of the prolyl *cis–trans* isomerization in the kinetics of folding and refolding and in protein stabilities. [24–32]. Despite the different kinetics for prolyl and non-prolyl isomerization, non-prolyl isomerization has been also known to be involved in the slow

* Corresponding author. Address: Departamento de Química, Universidad Nacional de San Luis, Chacabuco 917, 5700 San Luis, Argentina.
E-mail address: denriz@unsl.edu.ar (R.D. Enriz).

0022-2860/$ - see front matter © 2009 Elsevier B.V. All rights reserved.
doi:10.1016/j.molstruc.2009.06.027

steps for protein folding and refolding [32–34]. Peptide bond *cis*/*trans* isomerases have evolved to allow enzyme control switching backbone conformation in native proteins, folding intermediates, and unfolded chains. In addition, the intrinsic property of peptide bond *cis*/*trans* isomerases to decrease the internal barrier to rotation enhances the rotational flexibility around the targeted C—N bond, which in turn leads to backbone "liquificacion" localized to a "hot spot" protein region. In some cases, the slow rotational movement underlying peptide bond *cis*/*trans* isomerizations is found to control the biological activity of proteins. A comprehensive review on this topic has been reported by Fischer and Aumuller [35].

In spite of the importance of the *cis*-peptide bonds relatively little has been done theoretically on the subject. Previously we reported the 3D-Ramachandran map of formylglycinamide [9]. More recently we reported the conformational study of *cis* and *trans* *N*-formyl-*N*-methyl-L-glycin-*N*′-amide and *N*-acetyl-*N*-methyl-L-glycin-*N*′-methylamide using *ab initio* and DFT calculations [36]. In the present paper we report the *ab initio* and DFT conformational study of *cis*-peptide bonds of non-prolyl residues occurring in natural proteins. The present study aims to explore, characterize and present the geometric preferences of four *cis*-dipeptides: Ac-Gly-Gly-NHMe (**I**); Ac-Gly-Ala-NHMe (**II**), Ac-Ala-Gly-NHMe (**III**) and Ac-Ala-Ala-NHMe (**IV**) (Fig. 1). One of the goals of this paper is to compare the results of our theoretical calculations with previously reported experimental data obtained from X-ray analysis. Thus, the *cis* sequences: Gly124-Gly125 (present in Dihydrofolate reductase (*Pneumocystis carinii*))(PDB Code (1dyr)) [35]; Gly23-Ala24 (Glucoamylase-II) (PDB Code (1gai)) [38] and Ala74-Ala75 (Bacterial luciferase) (PDB Code (1luc) [39] were selected. We also include *cis*-Ala-Gly in the calculations in order to compare the conformational behaviour of this compound with those of the other non-prolyl *cis*-peptides reported here. An exhaustive electronic study employing the atoms in molecule (AIM) theory [40] was also carried out. Bader established the way to characterize the chemical bonds by the analysis of the electronic charge density in the bond critical points (BCPs). This methodology is used to establish the presence of hydrogen bonding in the different conformations of dipeptides in greater detail. It is an interesting approach which has been previously employed by our group on glutamate [41], glutamine [42] and isoleucine [43].

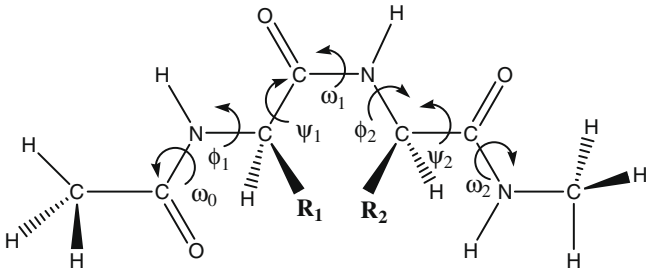

R_1 \ R_2	H	CH_3
H	**I** Gly—Gly	**II** Gly—Ala
CH_3	**III** Ala—Gly	**IV** Ala—Ala

Fig. 1. Skeletal diagram showing the torsion angles of compounds **I–IV**.

2. Methods of calculation

2.1. Nomenclature and Abbreviations

IUPAC-IUB [44] rules recommend the use of $0° \rightarrow +180°$ for clockwise rotation and $0° \rightarrow -180°$ for counterclockwise rotation. On the Ramachandran map (Fig. 2), the central box denoted by a broken line ($-180° \leqslant \Phi \leqslant 180°$) represents the cut suggested by the IUPAC convention. The four quadrants denoted by solid lines are the traditional cuts. Most peptide residues exhibit nine unique conformations, labelled as ad (α_{left}), ε_D, γ_D (C_7^{ax}), δ_L (β_2), (C_5), δ_D (α'), γ_L (C_7^{eq}), ε_L, and α_L (α_{right}). However, for graphical presentation of the conformational potential energy surface, we use the traditional cut ($0° \leqslant \Phi \leqslant 360$ and $0° \leqslant \varphi \leqslant 360°$), similar to that suggested previously by Ramachandran and Sasisekharan [1]. Refs. [9,36,41–43,45] give more details about these conformational codes.

In this study, four dipeptides (compounds **I–IV**) (Fig. 1) were investigated using molecular orbital computations. Thus, we are using the modular *N*- and C-protecting groups' approach whereby *N*-acetyl and *N*-methyl groups mimic the alpha carbons of the neighbouring amino acids in a polypeptide chain. Gly and Ala were chosen because they are the simplest amino acids with and without a side chain, which implies that it can be used as a template for the study of other amino acids.

2.2. Computations of molecular conformers

All the calculations were carried out using the Gaussian 03 program package [46]. In a first step, computations were carried out at the Restricted Hartree Fock/3-21G level of theory. The basis of this exploratory study was to identify the global and local minima of these four dipeptides on their respective Ramachandran maps. The importance of including electronic correlations in the conformational study has been previously reported [47]. Improta et al. [48] reported that conventional density functional theory (DFT) methods give an accurate description of both the geometry and the relative energy on these kind of molecular systems. Correlation effects were included in the present work using DFT with the

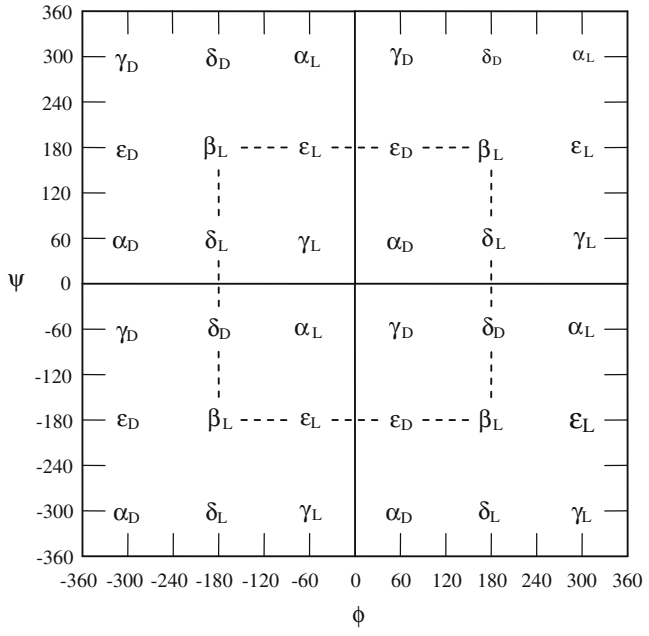

Fig. 2. Topological features of the Ramachandran map, $E = E(\Phi,\psi)$ associated with an aminoacid residue.

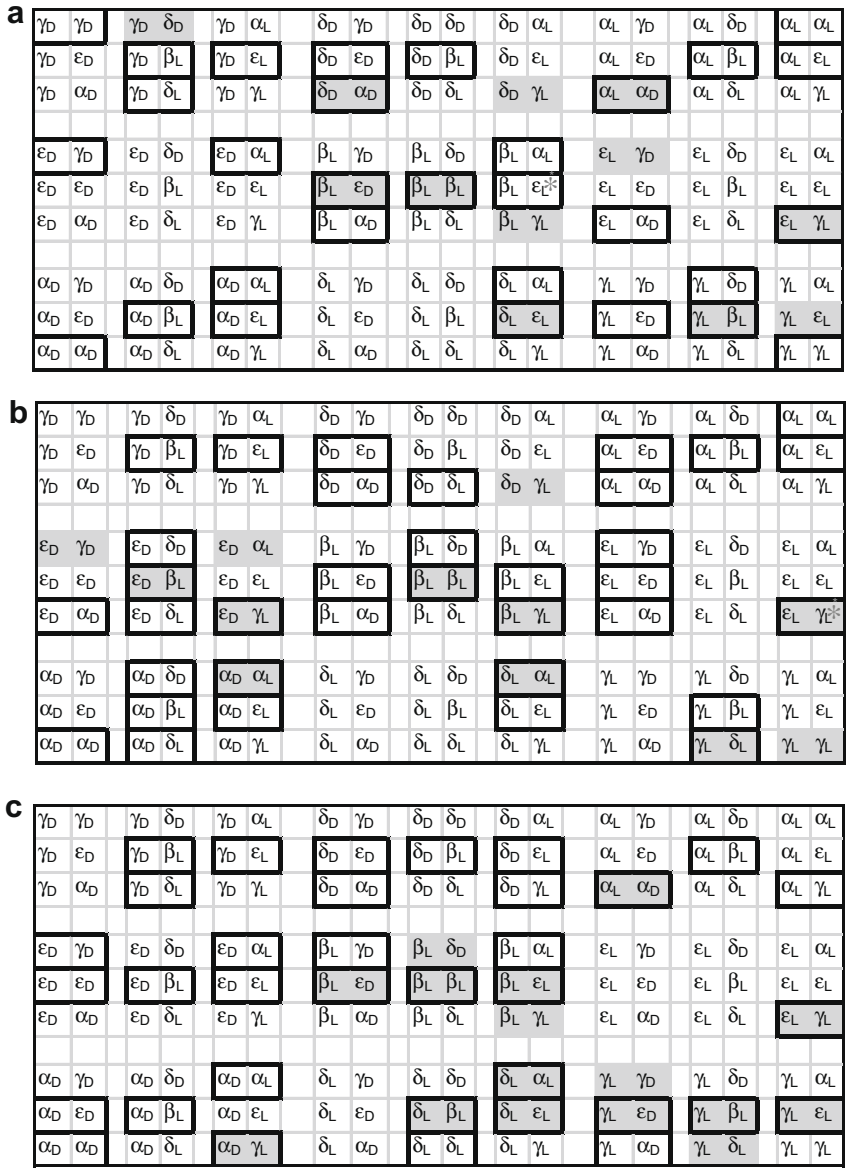

Fig. 3. Minima on the 4D-Ramachandran map of compound Ac-Gly-*cis*-Gly-NHMe (a), Ac-Gly-*cis*-Ala-NHMe (b), Ac-Ala-*cis*-Gly-NHMe (c) and Ac-Ala-*cis*-Ala-NHMe (d). Those conformers in bold rectangle are the conformers found from RHF/3-21G calculations, conformers in shaded grey are obtained from DFT calculations. The conformation obtained with X-ray diffraction is denoted with a red star.

Table 1
Torsional angles, total energies values, calculated relative energies (ΔE) of compound Ac-Gly-*cis*-Gly-NHMe optimized at B3LYP/6-31G(d) level of theory.

Topology		B3LYP/6-31G(d) E (hartree)	ΔE (kcal/mol)	ψ_0	ω_0	ϕ_1	ψ_1	ω_{CT}	ϕ_2	ψ_2	ω_2	ϕ_3
ε_L	γ_L	−664.5443676	0.00	147.51	167.39	293.95	149.53	0.25	267.06	30.71	176.16	239.80
γ_L	ε_L	−664.5439063	0.28	52.92	172.93	265.26	108.87	−17.28	247.25	121.69	182.15	239.01
β_L	β_L	−664.5430540	0.82	179.99	180.00	180.00	180.01	0.00	180.00	180.02	180.01	240.69
δ_D	γ_L	−664.5420107	1.48	12.59	172.86	121.57	288.77	9.02	280.20	119.69	179.34	240.37
β_L	γ_L	−664.5416040	1.73	233.03	183.93	171.82	176.14	5.56	262.72	3.49	180.26	240.67
β_L	ε_D	−664.5404158	2.48	227.85	180.33	189.56	172.39	15.80	76.12	156.95	175.50	240.67
γ_L	β_L	−664.5395972	2.99	225.14	187.02	240.87	59.83	5.01	146.89	198.36	182.85	240.77
ε_L	γ_D	−664.5389971	3.37	147.17	169.84	275.38	124.05	18.26	97.65	358.18	178.24	240.63
δ_D	α_D	−664.5384477	3.71	213.04	177.24	120.91	315.38	7.71	98.89	11.75	177.04	238.73
δ_L	ε_L	−664.5378336	4.10	217.14	180.77	204.74	52.26	2.74	263.28	220.21	183.48	238.73
γ_D	δ_D	−664.5372612	4.46	215.21	176.93	118.58	295.27	14.73	124.78	337.81	178.75	240.70
α_L	α_D	−664.5362296	5.11	296.33	186.55	289.61	326.82	9.39	97.29	13.92	182.86	240.04

Becke3-Lee-Yang-Parr (B3LYP) [49] functional and the 6-31G(d) basis set. The preferred conformations of each dipeptide derivative were optimized using B3LYP/6-31G(d) computations. An energy window of 5 Kcal/mol above the global minimum of each molecule

was considered to perform the DFT calculations. Thus RHF/3-21G geometry optimized structural parameters were used as the input in a subsequent theoretical refinement step with the inclusion of electron correlation effects at the B3LYP/6-31G(d) level of theory to obtain more reliable geometry and stability data.

N-acetyl and *N*-methylamide functionalities were added to the ends of the dipeptides as protecting groups to mimic the alpha carbon relationship in longer peptide chains. A standardized numbering system was used to define the molecules (Fig. 1) as it was numbered into and along the peptide backbone.

Multi-dimensional conformational analysis (MDCA) [50,51], a systematic method to predict the location of all minima as input *ab initio* calculations, was used to predict all topologically probable conformers. The Ramachandran PESs associated with a single amino acid has nine discrete possible conformations labelled as α_L, α_D, β, γ_L, γ_D, δ_L, δ_D, ε_L and ε_D. The topological arrangement of these minima and their defined dihedral angles are shown in Fig. 2. In addition to the dihedral angles, associated with the *cis–trans* peptide bonds (ω_0, ω_1 and ω_2), four torsional angles ($\Phi_1\Psi_1$, $\Phi_2\Psi_2$), were used as independent variables of the energy function

$$E = f(\Phi_1\Psi_1, \Phi_2\Psi_2) \quad (1)$$

In the case of dipeptide derivatives, each of the amino acids has nine conformers. Thus results in $9 \times 9 = 81$ legitimate conformations denoted in terms of subscript Greek letters.

2.3. Topological analysis of electron density

The topology of the electron density was analyzed using atoms in molecules theory (AIM) [40,52,53]. In this analysis, the gradient ($\Delta\rho$) and it Laplacian ($\Delta^2\rho$) play important roles. A critical point of

Table 2
Torsional angles, total energies values, calculated relative energies (ΔE) of compound Ac-Gly-*cis*-Ala-NHMe optimized at B3LYP/6-31G(d) level of theory.

Topology		B3LYP/6-31G(d) *E* (hartree)	ΔE (kcal/mol)	ψ_0	ω_0	ϕ_1	ψ_1	ω_{CT}	ϕ_2	ψ_2	ω_2	ϕ_3
γ_L	γ_L	−703.8623231	0.00	134.45	172.53	267.00	111.51	−13.85	244.00	112.94	183.06	240.32
ε_L	γ_L	−703.8606171	1.07	147.51	167.19	294.64	148.30	5.09	263.92	29.33	175.32	239.97
δ_D	γ_L	−703.8594372	1.81	135.54	171.85	122.20	290.34	−8.34	279.89	115.26	179.04	240.45
β_L	β_L	−703.8589435	2.12	121.85	179.20	180.82	181.61	1.05	209.23	153.21	176.93	240.59
β_L	γ_L	−703.8584889	2.41	223.12	184.66	170.61	175.20	6.67	262.22	2.00	179.80	240.62
ε_D	β_L	−703.8575230	3.01	218.49	192.19	105.04	214.47	12.98	194.31	156.26	176.24	240.78
ε_D	γ_D	−703.8566826	3.54	211.66	192.26	63.73	213.76	−11.58	78.71	356.05	180.68	239.76
ε_D	α_L	−703.8558169	4.08	130.11	185.87	85.45	235.50	19.71	263.16	359.48	181.61	240.59
ε_D	γ_L	−703.8558117	4.09	216.84	190.00	82.98	235.01	20.25	261.51	0.39	181.38	240.72
δ_L	α_L	−703.8551582	4.50	146.89	182.47	238.59	44.41	9.89	261.06	346.40	183.32	240.68
γ_L	δ_L	−703.8540126	5.21	142.40	182.64	242.51	68.32	18.60	229.29	24.52	179.36	240.63
α_D	α_L	−703.8530128	5.84	190.09	174.33	70.91	32.22	10.47	262.87	344.87	177.20	240.03

Table 3
Torsional angles, total energies values, calculated relative energies (ΔE) of compound Ac-Ala-*cis*-Gly-NHMe optimized at B3LYP/6-31G(d) level of theory.

Topology		B3LYP/6-31G(d) *E* (hartree)	ΔE (kcal/mol)	ψ_0	ω_0	ϕ_1	ψ_1	ω_{CT}	ϕ_2	ψ_2	ω_2	ϕ_3
ε_L	γ_L	−703.8609411	0.00	149.16	167.81	295.87	144.77	0.84	262.87	32.06	176.00	239.74
γ_L	β_L	−703.8593000	1.03	131.18	174.71	263.99	106.96	−8.52	208.53	161.65	178.80	238.66
β_L	β_L	−703.8585920	1.47	121.88	177.79	203.97	158.41	−10.89	187.41	182.09	180.74	240.70
γ_L	ε_D	−703.8574679	2.18	126.33	176.22	265.93	100.51	12.50	71.11	154.97	173.84	240.66
β_L	δ_D	−703.8568461	2.57	290.82	174.83	206.13	166.01	−15.35	121.57	347.09	180.60	240.63
β_L	γ_L	−703.8567575	2.63	237.28	179.37	203.04	155.11	−2.54	263.32	7.25	178.70	240.70
γ_L	ε_L	−703.8565212	2.77	264.43	170.21	254.9	93.84	−21.09	274.08	198.19	189.19	240.52
δ_L	β_L	−703.8565152	2.78	216.55	189.33	237.29	64.28	−1.05	153.66	198.13	183.21	240.76
γ_L	γ_D	−703.8562842	2.92	147.72	171.14	272.62	118.36	−14.04	95.28	358.88	177.35	240.78
β_L	ε_L	−703.8551382	3.64	130.96	175.25	201.95	165.91	−26.60	290.37	200.52	184.88	240.76
δ_L	ε_L	−703.8550153	3.72	335.16	179.62	208.30	60.55	−8.03	265.75	215.04	183.90	240.51
β_L	ε_D	−703.8549383	3.77	353.58	179.46	207.84	150.11	5.69	98.31	157.18	175.89	238.56
δ_L	α_L	−703.8548719	3.81	144.23	184.52	233.34	51.92	2.53	262.10	348.38	182.19	240.69
γ_L	δ_L	−703.8543739	4.12	132.27	185.16	240.43	73.01	9.10	235.94	25.96	179.03	240.82
α_D	γ_L	−703.8524871	5.30	203.93	170.04	48.16	52.04	4.85	241.12	17.87	178.37	240.30
α_L	α_D	−703.8524845	5.31	47.99	187.06	286.02	330.60	−7.76	96.91	12.60	184.38	240.62

Table 4
Torsional angles, total energies values, calculated relative energies (ΔE) of compound Ac-Ala-*cis*-Ala-NHMe optimized at B3LYP/6-31G(d) level of theory.

Topology		B3LYP/6-31G(d) *E* (hartree)	ΔE (kcal/mol)	ψ_0	ω_0	ϕ_1	ψ_1	ω_{CT}	ϕ_2	ψ_2	ω_2	ϕ_3
γ_L	γ_L	−743.1797400	0.00	123.15	175.29	266.10	109.50	−12.47	242.23	112.51	182.99	240.32
ε_L	γ_L	−743.1772136	1.59	149.95	167.51	296.08	143.09	5.74	258.03	33.58	175.36	239.79
β_L	γ_L	−743.1735709	3.87	109.79	180.55	201.91	155.26	−0.17	262.24	5.28	178.08	240.60
β_L	β_L	−743.1731812	4.12	122.11	176.59	206.26	163.29	−13.76	239.78	139.20	178.21	240.77
δ_L	α_L	−743.1715626	5.13	145.03	184.31	232.74	51.93	4.50	262.09	346.22	182.38	238.77
α_D	γ_L	−743.1688407	6.84	278.96	165.67	51.35	50.21	11.60	240.74	12.57	177.68	239.40

the electron density along the line of two interacting atoms in a molecule is called the bond critical point (BCP), where $\Delta\rho = 0$.

The bond path is made up of a pair of gradient paths, originating to a BCP and terminating at neighbouring nuclei. The necessary condition for two atoms to be bonded to each other is that their nuclei must be linked by a bond path. The bond path is regarded as "a universal indicator of bonded interaction" [54]. The method is widely used for proving the existence of hydrogen bonds [55].

3. Results and discussion

3.1. Conformational study

Ab initio molecular orbital computations were carried out on the putative 81 conformations of the four dipeptide models (**I–IV**) at the RHF/3-21G level of theory in order to determine the location of selected minima on their conformational potential energy hypersurfaces (PEHSs). The found minima are depicted in Fig. 3a–d. In contrast to the idealised topology, instead of 81, only 31, 35, 35 and 31 different conformations were found for compounds **I, II, III** and **IV**, respectively, (Fig. 3a–d). It should be noted that some conformations obtained at RHF/3-21G level, displayed relatively high energy with respect to the global minimum and therefore they are not significant from a thermodynamic point of view. In the next step of our study we optimized those conformations within an energy window of 5 Kcal/mol with respect to each global minimum using more accurate B3LYP/6-31G(d) calculations. Thus, 12, 12, 16 and 6 conformers were obtained at DFT level for compounds **I, II, III** and **IV**, respectively. These results are shown in Tables 1–4. Comparing the results shown in Fig. 3a–d and Tables 1–4, it is possible to obtain interesting general features. Both RHF/3-21G and B3LYP/6-31G(d) calculations predict a moderate but significant molecular flexibility for these compounds indicating that some conformational interconversions can take place without high energy requirements. However, there is also striking differences between the results obtained using these approaches. RHF/3-21G calculations predict the $\varepsilon_L\gamma_L$ conformation as the highly energetically preferred form for the four compounds reported here. These results indicate that for the RHF/3-21G calculations, the presence of the methyl group of Ala residues it is not relevant for the conformational preferences. In contrast, the B3LYP/6-31G(d) calculations predict the $\gamma_L\gamma_L$ conformation as the global minimum for compounds **II** and **IV** . This form was not found from RHF/3-21G optimizations. Interestingly, for compound **III**, the conformation $\varepsilon_L\gamma_L$ (the global minimum) possess a closely related spatial ordering to those of the $\gamma_L\gamma_L$ conformations of compounds **II** and **IV**, varying only the torsional angle ψ_1 in 24° (see

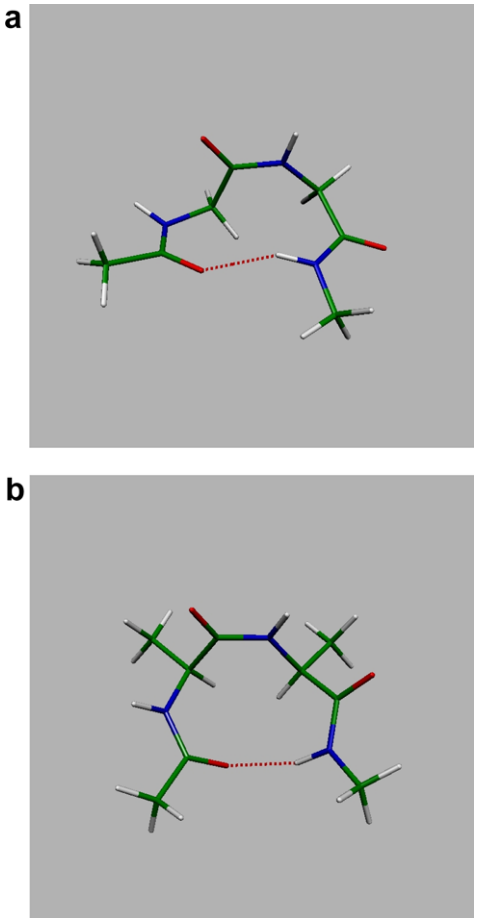

Fig. 4. Spatial view of the low-energy conformation obtained for (a) compound **I** ($\varepsilon_L\gamma_L$) and (b) compound **IV** ($\gamma_L\gamma_L$).

Table 5
Relative energies for the different conformations of compound **I–IV** obtained from single point. Calculations using aug-cc-pDVZ basis set.

Compound	Topology		*E* (hartree)	Δ*E* (kcal/mol)
I	β_L	β_L	−664.6464772	0.00
	ε_L	γ_L	−664.6463024	0.11
	γ_L	ε_L	−664.6452314	0.78
	β_L	γ_L	−664.6451217	0.85
	δ_D	γ_L	−664.6439470	1.59
	β_L	ε_D	−664.6431156	2.11
	γ_L	β_L	−664.6421502	2.72
	ε_L	γ_D	−664.6414599	3.15
	δ_D	α_D	−664.6397465	4.22
	γ_D	δ_D	−664.6393441	4.48
	δ_L	ε_L	−664.6390577	4.66
	α_L	α_D	−664.6379374	5.36
II	γ_L	γ_L	−703.9663549	0.00
	β_L	β_L	−703.9648693	0.93
	ε_L	γ_L	−703.9645652	1.12
	β_L	γ_L	−703.9643657	1.25
	δ_D	γ_L	−703.9639570	1.50
	ε_D	β_L	−703.9620630	2.69
	ε_D	α_L	−703.9608209	3.47
	ε_D	γ_L	−703.9607803	3.50
	ε_D	γ_D	−703.9604783	3.69
	δ_L	α_L	−703.9591713	4.51
	γ_L	δ_L	−703.9584970	4.93
	α_D	α_L	−703.9573626	5.64
III	ε_L	γ_L	−703.9660838	0.00
	γ_L	β_L	−703.9642750	1.14
	β_L	β_L	−703.9642011	1.18
	β_L	γ_L	−703.9628443	2.03
	β_L	δ_D	−703.9620516	2.53
	γ_L	ε_D	−703.9618623	2.65
	δ_L	β_L	−703.9615159	2.87
	γ_L	γ_D	−703.9612040	3.06
	γ_L	ε_L	−703.9605005	3.50
	β_L	ε_L	−703.9601515	3.72
	β_L	ε_D	−703.9600994	3.76
	γ_L	δ_L	−703.9589983	4.45
	δ_L	α_L	−703.9586796	4.65
	δ_L	ε_L	−703.9584061	4.82
	α_L	α_D	−703.9568304	5.81
	α_D	γ_L	−703.9557323	6.50
IV	γ_L	γ_L	−743.2862796	0.00
	ε_L	γ_L	−743.2843987	1.18
	β_L	γ_L	−743.2819667	2.71
	β_L	β_L	−743.2816636	2.90
	δ_L	α_L	−743.2782556	5.04
	α_D	γ_L	−743.2744837	7.40

Tables 2–4). From these results it appears that DFT calculations predict that the methyl group causes a moderated but significant disturbance of rotamers populations. The marked influence on rotational barriers which alter considerably the energy gaps among the conformers might be the responsible of these results.

It should be note that the $\gamma_L\gamma_L$ forms are folded conformations possessing an internal hydrogen bond which is stabilising this spatial ordering (Fig. 4b). The same observation is also valid for the $\varepsilon_L\gamma_L$ conformations (Fig. 4a).

The torsional angle ω_{C-T} (Fig. 1), which determine the *cis–trans* character of the peptide bond, displayed an average value of 5.93° (SD = 9.3), 5.41° (SD = 11.3), −5.02° (SD = 10.9) and −0.76 (SD = 10.2) for compounds **I**, **II, III** and **IV**, respectively. High resolution X-ray data obtained from 43 *cis*-peptide bonds of non-proline residues, displayed a value of 1.6° (SD = 4.7) (54) for this angle. Thus, both experimental data and theoretical calculations indicate that this torsional angle it is not totally planar, but very close to the planarity.

Table 5 gives the energy gaps obtained for the different conformations of compounds **I–IV** from more accurate calculations using an extended and flexible basis set. These results, in general are in agreement with the DFT results being the main difference the global minimum obtained for compound **I**. B3LYP/aug-cc-pVDZ// B3LYP/6-31G(d) calculations predict that the β_L, β_L form is the energetically preferred conformation. However, it should be noted that the energy gap obtained between the $\beta_L\beta_L$ and $\gamma_L\gamma_L$ conformations are expected to be populated significantly.

A comprehensive conformational analysis for For-Ala-t-Ala-NH_2 has been previously reported from *ab initio* calculations [45]. Thus, it is possible to perform some comparisons between those previous results with our data obtained for Ac-Ala-c-Ala-NMe. It has been proposed that the preceding or following diamide unit can stabilize the α_L and ε_L conformations, as substructures, which were found to be intrinsically unstable geometries in the For-Ala-NH_2. Our results indicate that the same appreciation is also valid for the Ac-Ala-c-Ala-NMe molecule. (Note that α_L and ε_L are stable forms for some conformers of (**I–IV**) Table 1–4.

At this stage of our work some general observations can be made with respect to the conformational intricacies of compounds I–**IV**. DFT and B3LYP/aug-cc-pVDZ// B3LYP/6-31G(d) calculations indicate that the energetically preferred conformations of these compounds are slightly influenced by the presence of the methyl groups of Ala residues. Also observing the energetically preferred conformations it is evident that the preferred forms are stabilized by internal hydrogen bonds. To understand better the above results, a detailed electronic study using AIM theory was carried out. The purpose was to obtain more precise information about the intramolecular interactions which are stabilising the different spatial orientations adopted by compounds **I–IV**.

3.2. Intramolecular interactions

An alternative method to analyze hydrogen bonding involves the topological analysis of electronic density distribution, which can be used to analyze intramolecular hydrogen bonding between H and a nearby heteroatom (Y) to gain some insight into the effect of hydrogen bond interactions on the conformations of dipeptides.

Table 6 shows the most significant topological local properties geometrical properties (interatomic distances and interaction angles), electron density (ρ); Laplacian of the electron density ($\Delta^2\rho$), ellipticity (ε), cocient between the Lagrangian of kinetic energy and electronic density (G/ρ) and total energy density (E_d) for the most representative structures obtained for compounds **I–IV**. The topological local properties reported correspond to the bond critical points from X—H···Y, where H represents the hydrogen atom involved in the bond.

All the BCPs (Bound Critical Points) found present two negative eigenvalues (λ_1 and λ_2) and one positive (λ_3) corresponding to a (3, −1) BCP type. All the geometries of these hydrogen bonds correspond to a length bond H···Y in the order of 1.98–2.4 Å; whereas

Table 6
Topological properties at hydrogen bond critical points of the most representative structures four compounds **I–VI**.

Dipeptido	Topologia[a]	PCE[b]	Interaction	Distancia[c] H—Y	Angulo[d] X-H—Y	100ρ[e]	$100\ \Delta_2\rho$[f]	100ε[g]	G/ρ[h]	$100E_d$[i]
Gly-Gly	ε_L–γ_L	(3, −1)	$O_7\cdots H_{15}$—N_{12}	2.02	154.50	2.2342455	7.1908644	0.4958585	0.8180975	−1.8278307
	γ_L–ε_L	(3, −1)	$O_7\cdots H_{15}$—N_{12}	2.05	153.80	2.0456803	6.8245813	4.1444786	0.8344408	−1.7069992
	δ_D–γ_L	(3, −1)	$O_7\cdots H_{15}$—N_{12}	2.06	163.10	2.0247774	6.5261895	2.4546673	0.8160893	−1.6523991
	δ_L–ε_L	(3, −1)	$N_3\cdots H_{16}$—O_{13}	2.04	143.70	2.3229329	7.3250046	4.7898603	0.8118946	−1.8859766
Gly-Ala	γ_L–γ_L	(3, −1)	$O_7\cdots H_{15}$—N_{12}	2.02	158.20	2.1474172	7.1399763	4.6356027	0.8343616	−1.7917225
	ε_L–γ_L	(3, −1)	$O_7\cdots H_{15}$—N_{12}	2.04	151.80	2.1419979	6.9204352	0.8064128	0.8190712	−1.7544487
	δ_D–γ_L	(3, −1)	$O_7\cdots H_{15}$—N_{12}	2.05	164.70	2.0797652	6.6468998	2.1335714	0.8128372	−1.6905105
	ε_D–γ_D	(3, −1)	$O_7\cdots H_{15}$—N_{12}	2.06	144.40	2.0979814	6.8882508	3.1961317	0.8273006	−1.7356613
	ε_D–α_L	(3, −1)	$O_7\cdots H_{23}$—C_{10}	2.40	152.10	1.1720980	3.7388103	7.8036460	0.7524715	−0.8819704
Ala-Gly	ε_L–γ_L	(3, −1)	$O_7\cdots H_{15}$—N_{12}	1.98	157.00	2.4210852	7.8648054	0.2626916	0.8244756	−1.9961257
	γ_L–β_L	(3, −1)	$O_7\cdots H_{23}$—C_{10}	2.22	159.90	1.7088962	5.1106183	5.3481926	0.7548054	−1.2898840
	γ_L–ε_D	(3, −1)	$O_7\cdots H_{19}$—C_{10}	2.28	152.30	1.4945469	4.5863546	5.9533379	0.7562376	−1.1302326
	γ_L–γ_D	(3, −1)	$O_7\cdots H_{19}$—C_{10}	2.35	152.00	1.2772238	4.0749814	7.5767855	0.7617200	−0.9728870
	δ_L–ε_D	(3, −1)	$N_3\cdots H_{16}$—O_{13}	2.10	138.70	2.0586540	6.6407175	7.2706400	0.8170252	−1.6819721
	γ_L–δ_L	(3, −1)	$O_7\cdots H_{23}$—C_{10}	2.30	152.30	1.4227843	4.4851052	6.6173904	0.7669879	−1.0912583
	α_D–γ_L	(3, −1)	$O_7\cdots H_{15}$—N_{12}	2.23	141.40	1.4265005	4.9698342	9.8841582	0.8349337	−1.1910333
Ala-Ala	γ_L–γ_L	(3, −1)	$O_7\cdots H_{15}$—N_{12}	2.02	158.40	2.1585244	7.1248049	4.5823509	0.8326550	−1.7973061
	ε_L–γ_L	(3, −1)	$O_7\cdots H_{15}$—N_{12}	1.99	155.30	2.3614329	7.6744832	0.2055672	0.8243803	−1.9467187
	α_D–γ_L	(3, −1)	$O_7\cdots H_{15}$—N_{12}	2.31	137.80	1.2232017	4.4068638	16.1099643	0.8400465	−1.0275464

[a] Obtained from MDCA.
[b] Critical point range of 0···H bond.
[c] Interatomic distance (A).
[d] Interaction angle (degrees).
[e] Electronic density.
[f] Laplacian of the electronic density.
[g] Ellipticity.
[h] Cocient between the lagrangian of kinetic energy and electronic density.
[i] Total energy density.

the bond angles X—H···Y range from 137.8° to 164.7°. According to the scheme elaborated by Popelier [52], the characterization of intra- and/or inter-molecular interactions, two criteria must be obeyed: (1) besides the proton donor, the acceptor center for positive charge must contain a minimum level of electron density (ρ), and (2) typical values for the Laplacian descriptor of charge density ($\Delta^2\rho$) must be carefully interpreted. The laplacian descriptors lead to consider $\Delta^2\rho < 0$ and $\Delta^2\rho > 0$ when covalent bonds (shared) or inter-/intra-molecular (closed-shell) contact are present [52], respectively. On another hand, Popelier [52] and Bader [53] proposed the existence of hydrogen bonding within the AIM formalism when ρ and $\Delta^2\rho$ at the BCP of two hydrogen bonded atoms are in the range of $0.002 \leqslant \rho \leqslant 0.035$ and $0.024 \leqslant \Delta^2\rho \leqslant 0.139$ a.u., respectively.

It is evident from the values listed in Table 6 that the representative structures obtained for compound **I–IV** fall into the common accepted range for hydrogen bonds mentioned above [53]. From Table 6 one can see some important points. O···H—N bonds with having suitable topological parameters at its BCP, namely: $0.0202 \leqslant \rho \leqslant 0.0242$, $0.0496 \leqslant \Delta^2\rho \leqslant 0.0786$ and $0.0020 \leqslant \varepsilon \leqslant 0.0988$, can make strong hydrogen bond interaction in comparison with other HBs. It is interesting to note that the topological properties at the O···H—N BCP for the $\alpha_D\gamma_L$ conformation of compound **IV** (namely: $\rho = 0.0122$, $\Delta^2\rho = 0.0440$ and $\varepsilon \leqslant 0.1610$, respectively) do not fall within the previous mentioned range, indicating a loose stabilization of this conformer by intramolecular HB. Topological values for O···H—C HBs are: $0.0117 \leqslant \rho \leqslant 0.0170$, $0.0373 \leqslant \Delta^2\rho \leqslant 0.0511$ and $0.0534 \leqslant \varepsilon \leqslant 0.0780$; these values shows low charge density and high ellipticity indicating weak interaction at these BCP.

The strength of these interactions might be well appreciated in Fig. 5. In this figure we plotted bond length vs. total energy density (E_d) and electronic density (ρ), respectively, as well. We can observe in this figure that the stronger interaction energies correspond to the shorter bond lengths and the higher electrostatic density. In other words, while the distance between the atoms decrease, stronger is the interaction and therefore the electrons are more localized.

Fig. 6 gives the contour map of $\Delta^2\rho$ obtained for the electronic density of the $\varepsilon_L\gamma_L$ conformation of compound **IV** calculated at B3LYP/6-31G(d) level of theory. Solid lines show rich-charged zones (ρ values lower than 0.0), whereas the poor-charged regions (ρ values higher than 0.0) are denoted by dot lines. The interatomic bonds are shown in green in this figure. The crossover between the interatomic surfaces and the plot plane are also in this Fig. 6. In addition, the BCP (3, −1) position is denoted by a double asterisk showing the corresponding hydrogen bond.

Fig. 7 displays the contour map of the $\Delta^2\rho$ obtained for the electronic density of the γ_L,β_L conformation of compound **III** calculated at B3LYP/6-31G(d) level of theory. We display here only two contour maps of the most representative forms. These results account for the general characteristics shown in Table 6. Different plots have been obtained for the rest of the conformations, with these results being considered representative of the overall phenomenon.

3.3. Correlation between natural occurrence of conformers and computed stability

The validity of this type of calculations may be assessed, at least in part, by comparing the predicted structure with that derived

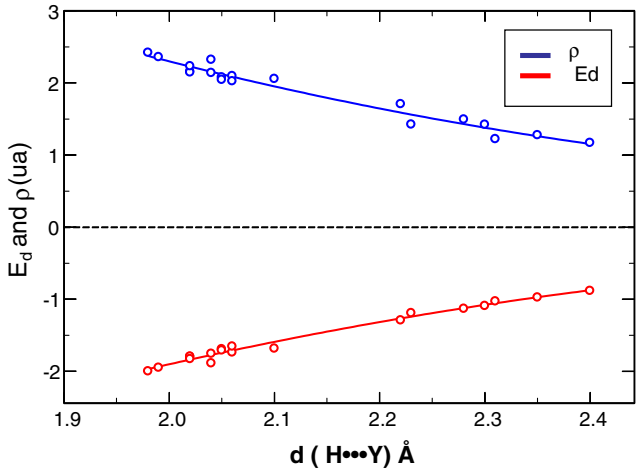

Fig. 5. Relationships obtained between: electronic density (ρ) versus distance (upper); and total energy density (E_d) versus distance (bottom).

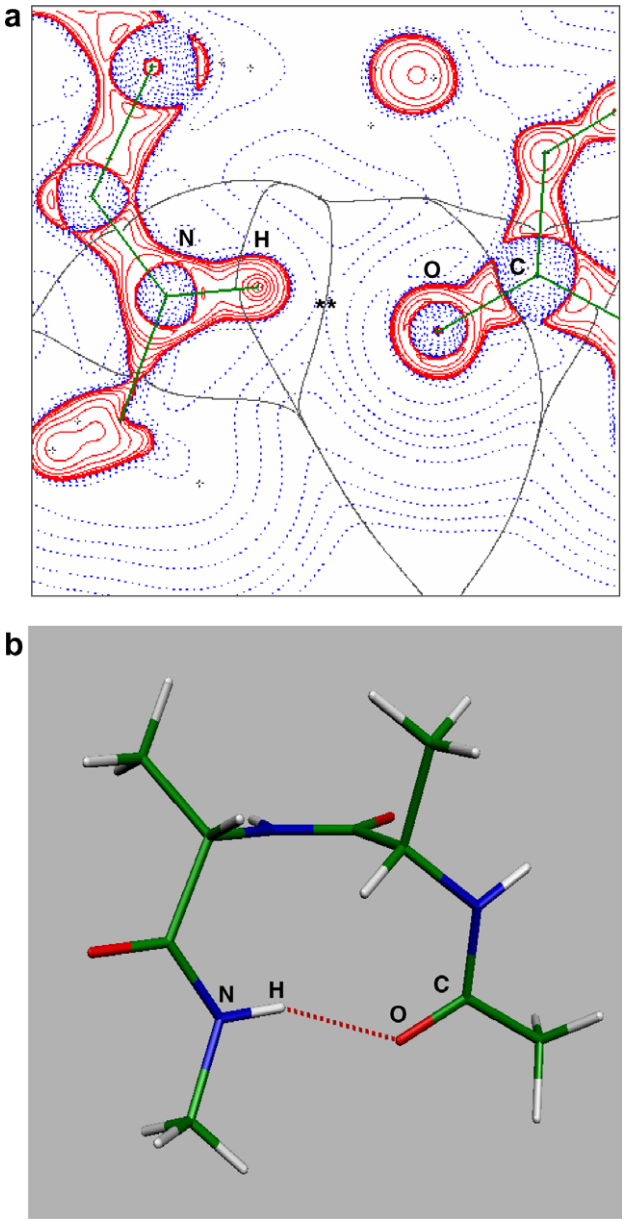

Fig. 6. (a) Contour map obtained for the laplacian of electronic density for the $\varepsilon_L\gamma_L$ form of compound **I**. This figure was plotted considering the N—H···O interaction and the values were obtained from B3LYP/6-31G(d) calculations. (b) Spatial view of the conformation used for the AIM theory analysis.

experimentally by X-ray crystallographic studies [37–39]. Thus, the comparison of the preferred forms obtained from theoretical calculations with the spatial orderings reported from X-ray data is possible for this cross-validation. We will assume that the probability of conformers in proteins depends only on its relative energy. This is a model in which several stabilizing factors are neglected, such as interresidue interactions, long-range effects, and hydration, among others. Acknowledging the limitations of this approach, the relative energy of a conformer can be correlated with the relative probability of the same backbone structure in an ensemble of proteins with known X-ray structures. Fig. 8 gives a comparison between the energetically preferred forms obtained from DFT calculations with those attained from X-ray data. The root main square deviation (RMSD) obtained between compounds I, II and IV with their experimental data are: 0.58 Å, 0.37 Å and 1.15 Å, respectively. The comparison of these conformations shows an emerging promising similarity.

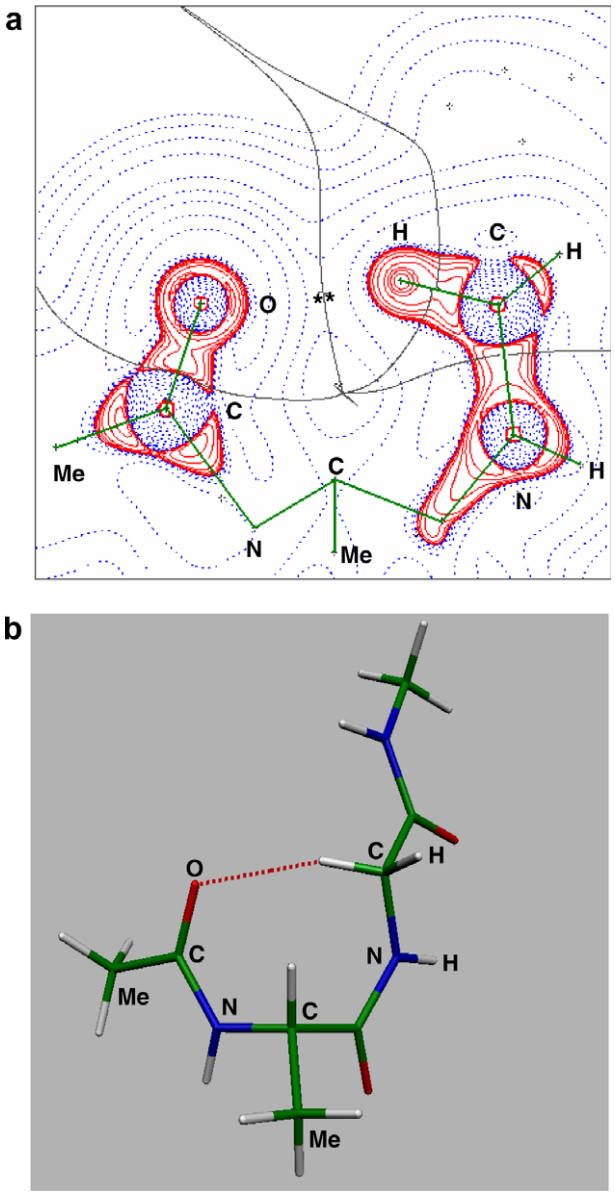

Fig. 7. (a) Contour map obtained for the laplacian of electronic density for the $\gamma_L\gamma_L$ form of compound **III**. This figure was plotted considering the C—H···O interaction and the values were obtained from B3LYP/6-31G(d) calculations. (b) Spatial view of the conformation used for the AIM theory analysis.

4. Conclusions

We report here the PEHSs of compounds **I–IV**. Thus, the conformational preferences of these compounds have been determined by theoretical calculations at different levels of theory. In general, the different calculations reported here RHF/3-21G, B3LYP/6-31G(d) and B3LYP/aug-cc-pVDZ//B3LYP/6-31G(d) displayed qualitatively similar results indicating that RHF computations using a modest basis set like 3-21G are sufficient to realize an exploratory and preliminary conformational analysis. However, higher levels of theory that consider the electronic correlation are necessary to confirm critical points and assign the conformational preferences. This is in particular apparent after examining that the energy gaps observed are different according to the employed levels of theory. Also the global minimum obtained for some compounds varies in function of the method used.

Using topological analysis of the electron density, we found hydrogen bonds, which stabilize the different conformers of compounds **I–IV**. On the basis of our results it appears that the Bader-type analysis gives a better understanding of the electronic structure showing the utility of this method of calculation to investigate the electronic structure of *cis*-dipeptides.

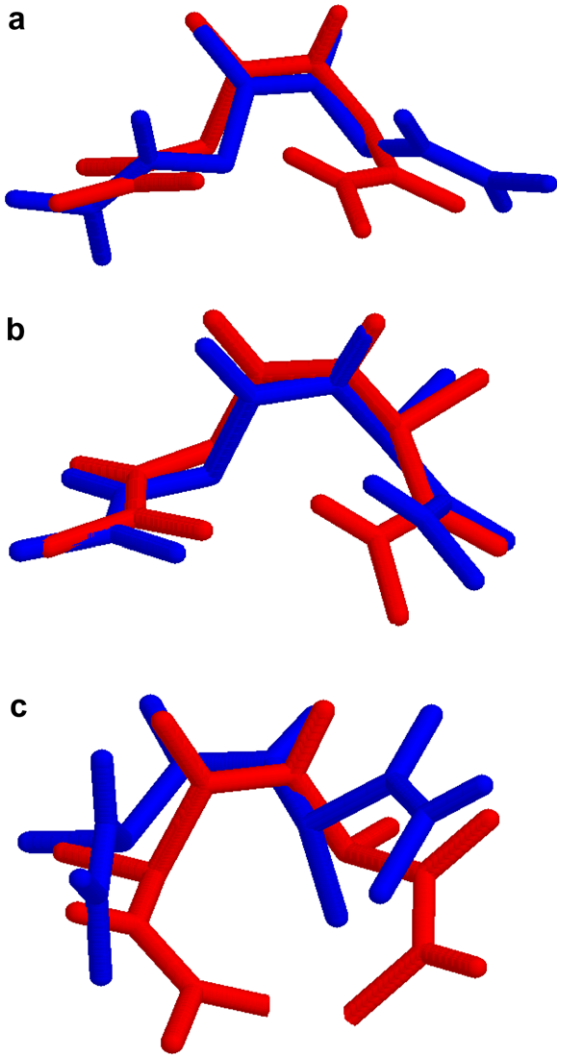

Fig. 8. Overlapped stereoview of the backbone conformations obtained from X-ray diffraction (blue) and conformations attained from DFT calculations (red). Compound **I** (a), coumpound **II** (b) and compound **IV** (c).

The conformations energetically preferred obtained for compounds **I**–**IV** are reasonably consistent with the experimental values obtained from X-ray. We believe that this study can contribute to a better understanding of some less noticeable effects, which might strongly influence the conformational preferences of these *cis*-dipeptides.

Acknowledgements

Grants from Universidad Nacional de San Luis (UNSL) supported this work. Part of this research was conducted using the resources of the IMASL, which receives funding from the National Research Council of Argentina (CONICET). R.D.E. and H.A.B. are members of the National Research Council of Argentina (CONICET-Argentina) staff.

References

[1] G.N. Ramachandran, V. Sasisekharan, Advan. Prot. Chem. 23 (1968) 283.
[2] L.A. La Plance, M.T. Rogers, J. Am. Chem. 23 (1968) 283.
[3] M. Perricaudet, A. Pullman, Int. J. Pept. Protein Res. 5 (1973) 99.
[4] D.H. Chistensen, N.R. Kortzeborn, B. Bak, J.J. Led, J. Chem. Phys. 53 (1970) 3912.
[5] D.M. Schnur, Y.H. Yun, D.R. Dalton, J. Org. Chem. 54 (1989) 3779.
[6] A. Radzicka, L. Pedersen, R. Wolfenden, Biochemistry 27 (1988) 4538.
[7] L.W. Jorgensen, J. Gao, J. Am. Chem. 110 (1988) 4212.
[8] Y.K. Kang, J. Phys. Chem. B 110 (2006) 21338.
[9] H.A. Baldoni, G.N. Zamarbide, R.D. Enriz, E.A. Jauregui, O. Farkas, A. Perczel, S.J. Salpietro, I.G. Csizmadia, J. Mol. Struct. 500 (2000) 97.
[10] R.D. Enriz, M.E. Morales, M.L. Freile, H.A. Baldoni, J. Argent. Chem Soc. 94 (2006) 1.
[11] G. Pohl, A. Perczel, E. Vass, G. Magyarfalvi, G. Tarczay, Tetrahedron 64 (2008) 2126.
[12] F.X. Schmid, L.M. Mayr, M. Müke, E.R. Schönbrunner, Adv. Protein Chem. 44 (1993) 25.
[13] J. Baldach, F.X. Schmid, in: R.H. Pain (Ed.), In Mechanisms of Protein Folding, second ed., Oxford University Press, New York, 2000 (chapter 8).
[14] W.J. Wedemeyer, E. Welker, H.A. Scheraga, Biochemistry 41 (2002) 14637.
[15] C. Dugave, L. Demange, Chem. Rev. 103 (2003) 2475.
[16] F.X. Schmid, R.L. Baldwin, Proc. Natl. Acad. Sci. USA 75 (1978) 4764.
[17] K.H. Cook, F.X. Schmid, R.L. Baldwin, Proc. Natl. Acad. Sci. USA 76 (1979) 6157.
[18] M.S. Weiss, A. Jabs, R. Hilgenfeld, Nat. Struct. Biol. 5 (1998) 676.
[19] S.S. Zimmerman, H.A. Scheraga, Macromolecules 9 (1976) 408.
[20] J.D. Gary, S. Clarke, Prog. Nucleic Acid Res. Mol. Biol. 61 (1998) 65.
[21] M.S. Strom, D.N. Nunn, S. Lory, Methods Enzymol. 235 (1994) 527.
[22] M. Ramek, A.M. Kelterer, S. Nikolic, Int. J. Quantum Chem. 65 (1997) 1033.
[23] S.G. Stepanian, I.D. Reva, E.D. Radchenko, L. Adamowicz, J. Phys. Chem. A 105 (2001) 10664.
[24] D.A. Schultz, F.X. Schmid, R.L. Baldwin, Protien Sci. 1 (1992) 917.
[25] C. Odefey, L.M. Mayr, F.X. Schmid, J. Mol. Biol. 245 (1995) 69.
[26] R.W. Dodge, H.A. Scheraga, Biochemistry 35 (1996) 1548.
[27] W.F. Walkenhorst, S.M. Green, H. Roder, Biochemistry 36 (1997) 5795.
[28] K. Maki, T. Ikura, T. Hayano, N. Takahashi, K. Kuwajima, Biochemistry 38 (1999) 2213.
[29] R. Golbik, G. Fischer, A.R. Fersht, Protein Sci 8 (1999) 1505.
[30] A. Cao, E. Welter, H.A. Scheraga, Biochemistry 40 (2001) 8536.
[31] G. Pappenberger, H. Aygün, J.W. Enjels, U. Reimer, G. Fischer, T. Kiefhaber, J. Mol. Biol. 8 (2001) 452.
[32] G. Pappenberger, A. Bachmann, R. Müller, H. Aygün, J.W. Enjels, T. Kiefhaber 326 (2003) 235.
[33] A.K.E. Svensson, J.C. O'Neill, C.R. Matthews, J. Mol. Biol. 326 (2003) 569.
[34] D.E. Stewart, A. Sarkar, J.E. Wampler, J. Mol. Biol. 214 (1990) 253.
[35] G. Fischer, T. Aumuller, Rev. Physiol. Biochem. Pharmacol. 148 (2003) 105.
[36] R.D. Enriz, M.E. Morales, H.A. Baldoni, J. Mol. Struct. 731 (2005) 177.
[37] J.N. Champness, A. Achari, S.P. Ballantine, P.K. Bryant, C.J. Delves, D.K. Stammers, Structure 2 (1994) 915.
[38] A.E. Aleshin, B. Stoffer, L.M. Firsov, B. Svensson, R.B. Honzatko, Biochemistry 35 (1996) 8319.
[39] A.J. Fisher, T.B. Thompson, J.B. Thoden, T.O. Baldwin, I. Rayment, J. Biol. Chem. 271 (1996) 21956.
[40] R.F.W. Bader, Atoms in Molecules. A Quantum Theory, Oxford University Press, Oxford, UK, 1990.
[41] M.F. Masman, M.A. Zamora, A.M. Rodriguez, N.G. Fidanza, N.M. Peruchena, R.D. Enriz, I.G. Csizmadia, Europ. Phys. J. D 20 (2002) 531.
[42] M.W. Klipfel, M.A. Zamora, A.M. Rodriguez, N.G. Fidanza, R.D. Enriz, I.G. Csizmadia, J. Phys. Chem. A 107 (2003) 5079.
[43] A.M. Rodriguez, J.C.P. Koo, D. Rojas, N. Peruchena, R.D. Enriz, Int. J. Quantum Chem. 106 (2006) 1580.
[44] IUPAC-IUB Commission on Biochemical Nomenclature, Biochemistry 9 (1970) 3471.
[45] A. Perczel, M.A. Mcallister, P. Csàszàr, I.G. Csizmadia, Can. J. Chem. 72 (1994) 2050.
[46] M.J. Frisch, G.W. Trucks, H.B. Schlegel, G.E. Scuseria, M.A. Robb, J.R. Cheeseman, J.A. Montgomery, Jr., T. Vreven, K.N. Kudin, J.C. Burant, J.M. Millam, S.S. Iyengar, J. Tomasi, V. Barone, B. Mennucci, M. Cossi, G. Scalmani, N. Rega, G.A. Petersson, H. Nakatsuji, M. Hada, M. Ehara, K. Toyota, R. Fukuda, J. Hasegawa, M. Ishida, T. Nakajima, Y. Honda, O. Kitao, H. Nakai, M. Klene, X. Li, J.E. Knox, H.P. Hratchian, J.B. Cross, C. Adamo, J. Jaramillo, R. Gomperts, R.E. Stratmann, O. Yazyev, A.J. Austin, R. Cammi, C. Pomelli, J.W. Ochterski, P.Y. Ayala, K. Morokuma, G.A. Voth, P. Salvador, J.J. Dannenberg, V.G. Zakrzewski, S. Dapprich, A.D. Daniels, M.C. Strain, O. Farkas, D.K. Malick, A.D. Rabuck, K. Raghavachari, J.B. Foresman, J.V. Ortiz, Q. Cui, A.G. Baboul, S. Clifford, J. Cioslowski, B.B. Stefanov, G. Liu, A. Liashenko, P. Piskorz, I. Komaromi, R.L. Martin, D.J. Fox, T. Keith, M.A. Al-Laham, C.Y. Peng, A. Nanayakkara, M. Challacombe, P.M.W. Gill, B. Johnson, W. Chen, M.W. Wong, C. Gonzalez, J.A. Pople, Gaussian, Inc., Pittsburgh PA, 2003.
[47] C. Alemán, J. Puuiggalí, J. Phys. Chem. B 101 (1997) 3441.
[48] R. Improta, V. Barone, K.N. Kudin, G.E. Scuseria, J. Chem. Phys. 114 (2001) 2541.
[49] (a) A.D. Becke, Phys. Rev. A 38 (1988) 3098;
(b) C. Lee, W. Yang, R.G. Parr, Phys. Rev. B 37 (1988) 785.
[50] M.R. Peterson, I.G. Csizmadia, Prog. Theor. Org. Chem. 3 (1982) 190.
[51] I.G. Csizmadia, in: I.G. Csizmadia, J.D. Bertran (Eds.), New Theoretical Concept for Understanding Organic Reactions, Reidel, Dordrecht, Netherlands, 1989.
[52] P.L.A. Popelier, Atoms in Molecules. An Introduction, Pearson Education, Harlow, UK, 1999.
[53] R.J. Bader, Phys Chem A 102 (1998) 7314.
[54] (a) D. Whiterfield, T. Tang, J. Am. Chem. Soc. 115 (1993) 9648;
(b) U. Koch, P. Popelier, J. Phys. Chem. 99 (1995) 9747;
(c) D. Whiterfield, D. Lamba, T. Tangm, I. Csizmadia, Carbohydr. Res. 286 (1996) 17;
(d) J. Platts, S. Howardm, B. Bracke, J. Am. Chem. Soc. 118 (1996) 2726;
(e) D. Fang, P. Fabian, Z. Szekely, X. Fu, T. Tang, I. Csizmadia, J. Mol. Struct. 427 (1998) 243;
(f) P. Popelier, J. Phys. Chem. A 102 (1998) 1873.
[55] A. Jabs, M.S. Weiss, R. Hilgenfeld, J. Mol. Biol. 286 (1999) 291.